Communication in Physical Sciences, 2025, 12(8):2185-2198

Coordination Driven Design and Biological Potentials of Mixed-Ligand Complexes Containing Diphenylmethanonehydrazone with 1, 10-Phenanthroline

Bridget Kpomah, Emuejevoke Loveth Igue, and Oyinlola Akande
Received:21 September 2025/Accepted: 05 December 2025/Published: 13 December 2025
https://dx.doi.org/10.4314/cps.v12i8.2

Abstract : *Mn(II), Fe(II), Co(II), Ni(II) and Zn(II) complexes of diphenylmethanone hydrazone with 1, 10-phenanthroline as secondary ligand has been synthesized. All compounds were characterized through CHN micro-elemental analysis, melting point analysis, solubility analysis and spectroscopic analysis (FTIR and UV-visible). The results of partial elemental analysis are in agreement with assigned formulations, while melting points of the complexes are higher as compared to the derived ligand. Spectroscopic analysis results confirmed the coordination of diphenylmethanonehydrazone to the various center metals in bidentate fashion via the azomethine nitrogen (C=N) and the H-N-H amide group. Similarly, the secondary ligand; 1, 10- phenanthroline also produced a bidentate chelate with interactive metal ions using the heterocyclic imine (C=N) bands. All the results suggested octahedral geometry to the complexes and have $[M(L_1)(L_2)Cl_2]$, where L_1= diphenylmethanonehydrazone, L_2 = 1, 10-phenathroline and M = Mn(II), Fe(II), Co(II), Ni(II) and Zn(II). The IR spectra of the complexes were assigned and compared with the data in literature. In-vitro antifungal activity of these compounds was determined using our (4) pathogenic fungi (Aspergillus niger ATCC16404, Candida albicans ATCC10231, Trichoderma longibbrachiatum ATCC18648 and Rhizopus stolonifier ATCC14037). Both the derived ligand and the mixed-ligand complexes were active against fungal strains. The screening revealed an increased activity of the complexes against the fungal isolates compared to the free ligand. Fe(II) complex, showed highest activity among the complexes screened, however, other complexes displayed considerable antifungal activity.*

Keywords*: Synthesis, spectroscopy, hydrazone, diphenylmethanone, 1, 10-phenanthroline, antifungal activity*

Kpomah Bridget
Department of Chemistry, Delta State University, Abraka, Nigeria
Email: tressurekpomah@yahoo.com
Orcid id: 0000-0001-7350-2827

Igue Emuejevoke Loveth
Department of Chemistry, Delta State University, Abraka, Nigeria
Email: flourishvoke4real@gmail.com
Orcid id: 0009-0001-0093-3017

Akande Oyinlola
Department of Science Laboratory Technology, Federal Polytechnic Orogun, Delta State, Nigeria
Email: akande.oyinlola@fepo.edu.ng
Orcid id: 0009-0000-8844-0788

1.0 Introduction

Antimicrobial resistance (AMR) is currently a persistent global public health issue, causing a projected 10 million deaths annually worldwide by 2050 (Dadgostar, 2009). Therefore, the big challenge for public health is the development and/or implementation of effective strategies to decrease the emergence and spread of antimicrobial resistance. This can only be achieved through the production of novel and successful anti-infective drugs that are safe for clinical therapy (Ventola 2015; Muteeb *et al*., 2023)

hydrazones have mounted as a key-skeleton for the development of active drugs, due to their important biological and pharmacological profiles, they are being manufactured as medicines by various investigators to fight against the ailments with maximal effects and minimal toxicity, they are organic compounds characterized by the presence of the $R_2C = NNHR$ group, which possess applications in organic synthesis, analytical chemistry and medicine (Borges *et al*., 2015; Swartz, 2000; Tegos and Hamblin 2013). A Schiff base is an organic compound containing an imine (azomethine) functional group —R–C=N–R'— formed by the condensation of a primary amine with an aldehyde or ketone. They are sometimes called azomethines and are widely used as ligands because the C=N unit can coordinate metal ions and tune electronic/steric properties (Ali *et al*., 2023) Schiff bases and other nitrogen-containing ligands have been employed as chelating agents in coordination chemistry; they were regarded as a crucial ligand class that forms a variety of metal complexes (Ali and Livingstone 1974; Jain *et al*., 2023; Kumar *et al*., 2023). Schiff-base ligands form stable complexes with many transition metals (3d block and beyond), and these metal–Schiff base complexes are extensively used as catalysts for oxidation, hydrogenation, C–C bond forming reactions, and more (Malay and Ray, 2025; Juyal *et al*., 2023). These metal complexes have numerous applications in various biological domains because the nitrogen atoms are in proximity, and the core ring maintains its rigid structure, allowing 1,10-phenanthroline to synthesize complexes with metal ions more efficiently (Lemire *et al*., 2013; Kpomah *et al*., 2024; Azab *et al*., 2015). In this study, spectroscopic techniques and thermal analysis were used to characterize the new Schiff base ligand: Diphenylmethanone hydrazone that resulted from the condensation reaction of hydrazine hydrate with diphenylmethanone. Mn(II), Fe(II), Co(II), Ni(II), and Zn(II) complexes of diphenylmethanonehydrazone were synthesized. Furthermore, 1,10-phenanthroline (phen) was used as a co-ligand with diphenylmethanonehydrazone to synthesize Mn(II), Fe(II), Co(II), Ni(II) and Zn(II) mixed-ligand complexes. The biological activities and the minimum inhibitory concentration (MIC) of the compounds were also reported.

2.0 *Materials and Methods*

All metal salts, solvents and other reagents used were of analytical grades. Hydrazine hydrates, diphenylmethanone, 1, 10-phenanthroline and acetic acid required for the synthesis were procured from Bristol Scientific Company. The metal salts used for the synthesis were obtained from British Drug House (BDH), they include: iron(II) chloride, Zinc(II) chloride, Nickel(II) chloride, manganese(II) chloride and cobalt(II) chloride. Methanol and ethanol were distilled before use; all reactions were monitored by silica gel pre-coated thin-layer chromatography (TLC). FTIR spectroscopy of the compounds were recorded on 5500 Series Compact FTIR spectrophotometer as KBr pellets in the range 4000 – 650 cm^{-1}. The absorptions were given in wave numbers (m^{-1}) Melting points were recorded on electrothermal melting point apparatus and are uncorrected. UV-visible spectroscopy of the complexes was run on SPECORD 200 plus UV-visible spectrophotometer in the range 200 – 700. CHN elemental analysis of the synthesized compounds was performed on EMA 502 elemental micro analyzer.

2.1 Synthetic Procedures

2.1.1 Synthesis of diphenylmethanonehydr - azone (DPMH)

To a stirred 30 mL ethanolic solution of (0.182 g, 1 mmol) was added two drops of 2 % acetic

acid. 30 mL ethanolic solution of hydrazine hydrate (0.05 mL, 1mmol) was added. The solution of diphenylmethanone and hydrazine hydrate in a ratio 1:1 was stirred until a homogeneous solution was obtained, which was refluxed and stirred for 6 hrs at 50 ^{O}C. Two drops of concentrated sulphuric acid were added to the resulting mixture. A light brown precipitate was formed. The precipitate was filtered and washed with ethanol several times to remove unreacted hydrazide; the product was then filtered and dried in a vacuum oven at 60 ^{O}C overnight. The synthesis of diphenylmethanonehydrazone was carried out by adapting the Azab methodology (Mihsen *et al*., 2020).

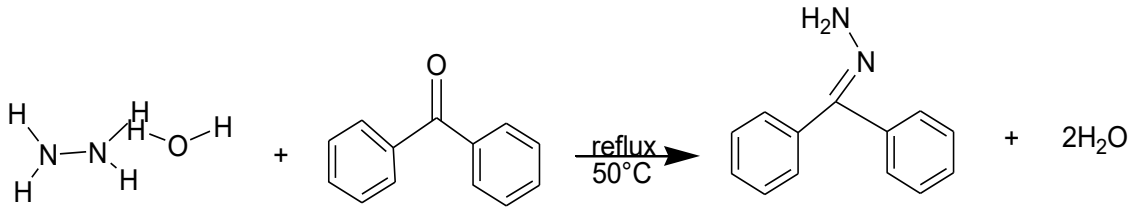

Scheme 1: Synthesis of diphenylmethanonehydrazone (DPMH)

2.1.2 Synthesis of 1, 10-phenanthroline diphenylmethanonehydrazone metal complexes

(0.195 g, 1 mmol) 30 mL of ethanolic diphenylmethanonehydrazone was prepared. Thereafter, (1 mmol) 30 mL ethanolic solutions of the respective metal salts were also prepared. diphenylmethanonehydrazone solution was added to each metal salt solution under magnetic stirring at 80 ^{O}C and reflux for about 1 hr. Consequently, (0.06 g, 1 mmol) 30 mL ethanolic solution of 1, 10-phenathroline was added. The resulted solution in ratio 1:1:1 was further stirred under at 80 ^{O}C and refluxed for another 4 hrs to allow the formation of 1, 10-phenanthroline diphenylmethanonehydrazone metal complex. The supernatant liquid was decanted while the residue was filter and dried in a vacuum oven at 60 ^{O}C. (Mihsen *et al*., 2020).

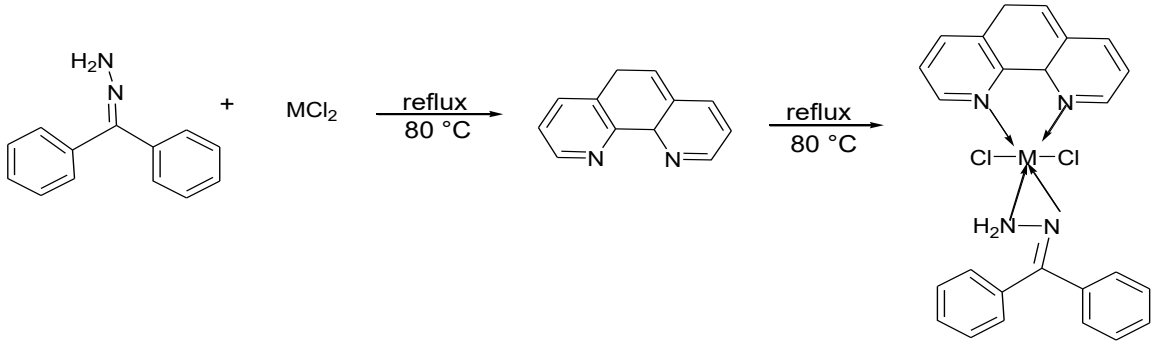

Schem 2: Synthesis of 1, 10-phenanthroline diphenylmethanonehydrazone metal complexes

3.0 *Characterization*

3.1.1 Elemental analysis

CHN elemental analysis of the synthesized compound was performed at Central Research Laboratories, University of Ilorin, Kwara State, on EMA 502 Elemental Micro Analyzer.

3.1.2 UV-visible spectroscopy

UV-visible spectroscopy of the complexes was run on SPECORD 200 plus UV-visible spectrophotometer in the range 200–700 nm available at Central Research Laboratories, University of Illorin, Kwara State. The sample solution was placed in a quartz cuvette of 1cm path length. Absorption wavelength of each

peak and the corresponding absorbance were displayed and recorded. The printout of spectra was obtained from the printer connected to the instrument via the computer system.

3.1.3 ***Infrared spectroscopy***

The IR spectra were recorded on 5500 series compact FTIR spectrophotometer as KBr pellets in the range 4000 – 650 cm^{-1} at Central Research Laboratories, University of Illorin, Kwara State. Small portions of the sample in solid form were ground with pure dry spectroscopic grade KBr. The powdered mixture was distributed evenly on a dyne and covered with a dyne lid. A pressure was exerted under vacuum for the mixture to form a disc. The disc was mounted directly in the sample beam path of the spectrophotometer and the spectrum was recorded.

3.2 ***Antimicrobial sensitivity test of the prepared compounds***

All the prepared metal complexes were tested against four (4) fungi strains; fungi (*Rhizopus stolonifier* ATCC 14037, *Aspergillus niger* ATCC16404, *Candida albicans* ATCC 10231 and *Trichoderma longibbrachiatum* ATCC 18648). The microorganisms were collected from Eku Teaching Hospital, Eku, Delta State. Confirmatory tests were carried out in the Pharmaceutical Microbiology Laboratory of the Faculty of Pharmacy, Delta State University, Abraka, each fungal strain was cultured in potato dextrose broth. The compounds were soluble in dimethylsulphoxide (DMSO). 0.1 mL of each fungal strain culture was utilized to inoculate the agar plates with swab sticks. The inoculation plates were appropriately labeled, and uniform wells were created using a 6 mm diameter plastic cork borer. 200, 100, and 50 mg/mL of each compound were dispensed into separate wells using a Pasteur pipette. fluconazole, ketoconazole, and intraconazole served as standard antifungal, all examined using identical methodologies. The plates were incubated for 48 hours at 28 ^{O}C for fungi; thereafter, the widths of the zones of growth inhibition (ZOI) were measured with a meter rule to the closest millimeter and then that of the antibiotic discs were scored as sensitive, intermediate susceptible and resistant according to the National Committee for Clinical Laboratory Standards (NCCLS) recommendations (≤ 13 = resistant; 14 to 15 = intermediately, susceptible; ≥ 16 = sensitive). The minimum inhibitory concentration (MIC) was calculated in µg/mL.

4.0 Results and Discussion

4.1 Physical and Analytical Characteristics

To evaluate the successful formation of the mixed-ligand complexes and to understand their fundamental physicochemical properties, the physical and elemental analytical data of the synthesized compounds were examined. These results are presented in Table 1, which summarizes the molecular weight, appearance, percentage yield, melting point, and elemental composition of the free ligands and their corresponding Fe(II), Zn(II), Ni(II), Mn(II), and Co(II) complexes.

The data in Table 1 show that all the metal complexes were obtained as crystalline solids with good to excellent yields ranging from 68% to 92%. The high yields indicate that the synthetic procedure is efficient and that the ligands (DPMH and phen) coordinate readily with the metal ions under the employed reaction conditions.

The colour variations of the complexes—orange-red for Fe(II), light brown crystals for Zn(II), Ni(II), and Co(II), and metallic light-brown powder for Mn(II)—reflect differences in the ligand field environment around each metal ion. These differences suggest metal-dependent changes in d–d transitions and charge-transfer characteristics, consistent with mixed-ligand coordination involving both

DPMH (a hydrazone ligand) and phen (a π-acceptor ligand).

The melting points of the complexes (316–396 °C) are significantly higher than those of their parent ligands (DPMH at 150 °C and phen at 117 °C). Such elevated melting points indicate increased thermal stability upon chelation. The Ni(II) complex shows the highest melting point (396 °C), suggesting a more rigid coordination environment or stronger metal–ligand bonding. The elemental analysis (C, H, N) shows close agreement between the calculated and experimentally found values, with variations falling within acceptable analytical limits. This confirms the proposed formulations and verifies that each metal center coordinates with one molecule each of DPMH and phen, together with two chloride ions. For example, the Fe(II) complex, $[Fe(L_1)(L_2)Cl_2]$, shows found carbon content of 57.78% compared to the calculated 59.43%, and similar correspondences appear for hydrogen and nitrogen. These results align well with the stoichiometry $C_{25}H_{22}Cl_2FeN_4$.

Table 1: Physical and analytical characteristics of 1, 10-phenanthroline diphenylmethanonehydrazone complexes

					Elemental analysis Found / (calcd) (%)		
Formulation and empirical formula	**M/WT (g/mol)**	**Colour/ Appearance**	**Yeild (%)**	**Melting point (°C)**	**C**	**H**	**N**
DPMH (L_1) ($C_{13}H_{12}N_2$)	196.10	Light brown powder	78	150	78.56 (79.56)	5.97 (6.16)	13.87 (14.27)
Phen (L_2) ($C_{12}H_8N_2.H_2O$)	180.21	Cream/solid	-	117	-	-	-
$[Fe(L_1)(L_2)Cl_2]$ ($C_{25}H_{22}Cl_2FeN_4$)	505.22	Orange-red crystals	77	336	57.78 (59.43)	4.96 (4.39)	10.54 (11.09)
$[Zn(L_1)(L_2)Cl_2]$ ($C_{25}H_{22}Cl_2N_4Zn$)	514.76	Light brown crystals	68	365	57.04 (58.33)	3.94 (4.13)	10.89 (10.88)
$[Ni(L_1)(L_2)Cl_2]$ ($C_{25}H_{22}Cl_2N_4Ni$)	508.07	Light brown crystals	78	396	57.84 (59.10)	3.89 (4.36)	11.24 (11.03)
$[Mn(L_1)(L_2)Cl_2]$ ($C_{25}H_{22}Cl_2MnN_4$)	504.32	Light brown metallic powder	92	324	58.78 (59.54)	4.96 (4.40)	10.54 (11.11)
$[Co(L_1)(L_2)Cl_2]$ ($C_{25}H_{22}Cl_2CoN_4$)	508.31	Light brown crystals	84	316	58.23 (59.07)	3.94 (4.36)	10.86 (11.02)

The molecular weights of the complexes (504–515 g/mol) further support the formation of heteroleptic mixed-ligand species. The systematic increase in molecular weight compared to the free ligands is consistent with the coordination of both ligands and chloride ions to the metal center.

The physical appearance and stability of the synthesized complexes, which remained stable in air and did not decompose under normal laboratory conditions, suggest successful chelation. The rigidity induced by the bidentate coordination of both ligands contributes to the observed stability.

Overall, the data presented in Table 1 confirm that the reaction of DPMH with 1,10-phenanthroline and the respective metal ions results in the successful formation of mixed-ligand complexes possessing well-defined physicochemical properties. The close match between theoretical and experimental elemental values, along with the high melting points and consistent colour characteristics, provide strong evidence for the proposed coordination environment and structural integrity of these compounds.

The solubility behaviour of the synthesized mixed-ligand complexes was examined to provide additional insight into their physicochemical characteristics, structural rigidity, and interaction with solvents of varying polarity. The solubility patterns of the Fe(II), Zn(II), Ni(II), Mn(II), and Co(II) complexes of DPMH and 1,10-phenanthroline are presented in Table 2, which shows their behaviour in protic and aprotic solvents under both cold and hot conditions.

Table 2: Solubility data for 1,10-phenanthroline diphenylmethanonehydrazone complexes. The results in Table 2 indicate that all the metal complexes exhibit similar solubility trends irrespective of the metal ion. Under cold conditions, the complexes are insoluble in distilled water, methanol, and ethanol, and only slight increases in solubility are observed when the solvents are heated. The inability of these protic solvents to dissolve the complexes, even at elevated temperatures, suggests that the complexes possess strong intermolecular interactions and structurally rigid coordination frameworks that resist disruption by weak or moderately polar solvents.

Table 2: Solubility data for 1, 10- phenanthroline diphenylmethanonehydrazone complexes

LIGAND /COMPLEX	DISTILLED WATER		METHANOL		ETHANOL		DMF		CHLOROFORM		DMSO	
	COLD	HOT	COLD	HOT	COLD	HOT	COLD	HOT	COLD	HOT	COLD	HOT
$[Fe(L_1)(L_2)Cl_2]$	NSC	SSH	NSC	SH	NSC	SH	SSC	SH	SSC	SH	SSC	SH
$[Zn(L_1)(L_2)Cl_2]$	NSC	SSH	NSC	SH	NSC	SSH	NSC	SSH	NSC	SSH	NSC	SSH
$[Ni(L_1)(L_2)Cl_2]$	NSC	NSH	NSC	SH	NSC	SSH	SSC	SH	SSC	SH	SSC	SH
$[Mn(L_1)(L_2)Cl_2]$	NSC	NSH	NSC	SH	NSC	SSH	SSC	SH	SSC	SH	SSC	SH
$[Co(L_1)(L_2)Cl_2]$	NSC	SSH	NCS	SSH	NSC	SSH	SSC	SH	SSC	SH	SSC	SH

In contrast, all the complexes show good solubility in DMF and DMSO, both under cold and hot conditions. These two highly polar aprotic solvents have strong donor abilities that favour the solvation of metal complexes containing multiple nitrogen donor atoms and aromatic systems. Their ability to dissolve the complexes readily indicates that the synthesized species possess polarity but require solvents with very high dielectric constants to overcome lattice energies and intermolecular forces. Chloroform shows moderate solubility for most complexes under hot conditions but limited solubility when cold. This intermediate behaviour aligns with the moderately polar nature of chloroform, which interacts only partially with the sterically hindered and aromatic-rich structure of the complexes.

The solubility patterns observed in Table 2 are consistent with the physical and analytical properties previously reported in Table 1. The high melting points of the complexes, which range from 316 to 396 °C, indicate the presence of strong metal–ligand bonds and compact coordination environments. These strongly bonded structures are inherently difficult to solvate in low-polarity or protic solvents, thereby explaining the poor solubility in water,

methanol, and ethanol. The crystalline and thermally stable nature of the complexes reported in Table 1 further supports the limited solubility in weak solvents. A rigid, aromatic, and multidentate coordination environment contributes to tight molecular packing and significant intermolecular forces, which protic solvents cannot effectively disrupt.

The elemental analytical data in Table 1 confirm the formation of heteroleptic complexes with DPMH and 1,10-phenanthroline acting as bidentate ligands. This multidentate mode of coordination produces bulky, neutral complexes that are more compatible with strong dipolar aprotic solvents such as DMF and DMSO. The aromatic rings in the ligands encourage pi–pi stacking interactions in the solid complexes, which further reduce solubility in protic solvents. The similar solubility behaviour of all the complexes reflects that they possess comparable coordination geometries and structural arrangements, as indicated by their closely matching analytical and physical data.

In summary, the solubility behaviour reported in Table 2 complements the physical and analytical characteristics presented in Table 1. Together, they confirm that the mixed-ligand complexes are structurally robust, thermally stable, and moderately polar species that dissolve readily only in solvents of high dielectric strength. The consistency between the thermal stability, elemental composition, appearance, and solubility behaviour provides strong evidence that the intended mixed-ligand complexes were successfully synthesized.

Table 3: Infrared spectroscopy for 1,10-phenanthroline diphenylmethanonehydrazone complexes.

The infrared spectral characteristics of the synthesized mixed-ligand complexes were examined to identify the functional groups involved in coordination and to compare the effects of metal binding on the vibrational frequencies of the ligands. The infrared bands recorded for DPMH, 1,10-phenanthroline, and their Fe(II), Zn(II), Ni(II), Mn(II), and Co(II) complexes are presented in Table 3. The assignments of IR band of 1, 10-phenanthroline diphenylmethanonehydrazone mixed ligand Fe(II), Zn(II), Ni(II) Mn(II) and Co(II) complexes are summarized in Table 3. The presence of C=C aromatic stretch were confirmed in the region 1561-1480 cm^{-1} which indicates a shift to a lower frequency. C-H aromatic stretch was confirmed by the presence of strong bands in the region of 3060-2877 $cm^{-1,}$ and it's the most common band amongst all the other bands with a shift to a higher frequency according to Zainab M. Hassan (Al-Shemary *et al*., 2016).

The V(H-N-H) band is found between 1650-1600 cm^{-1} and it's the band that indicates the presence of the hydrazinic band V(N-N) found between 1100-1000 cm^{-1} and its usually to a lower frequency when coordinated to metal salts. The free 1, 10-phenanthroline V(C=N) stretch is usually 1651 cm^{-1} but upon metal co-ordination, there was a shift to a lower wavelength. The IR spectra of the complexes were analyzed to identify the coordination sites potentially involved in chelation. Chelation is expected to modify these peak placements and/or intensities (Kashar and El-Sehli, 2013)

Table 3: Infrared spectra data (cm^{-1}) of 1, 10-phenanthroline diphenylmethanonehydrazone complexes

COMPOUND (MOLECULAR FORMULA)	IR BANDS						
	V(N-H)	V(C-H)	V(C=N)	V(C=C)	V(M-N)	V(H-N-H)	V(N-N)
DPMH (L_1)	3500	2877	1651	1561	-	1650	1025 1062
phen (L_2)		3035	1620				
$[Fe(L_1)(L_2)Cl_2]$	3420	3020 3030	1580	1480	590	1600	1010
$[Zn(L_1)(L_2)Cl_2]$	3268 3421	3060	1555	1500	600	1620	1025
$[Ni(L_1)(L_2)Cl_2]$ ($C_{25}H_{22}Cl_2N_4Ni$)	3306	3030 3060	1628	1465	609	1640	1010
$[Mn(L_1)(L_2)Cl_2]$	3400	3045	1590	1500	510	1620	1020
$[Co(L_1)(L_2)Cl_2]$	3420	3060	1636	1490	500	1620	1010

.Infrared bands move to higher or lower frequencies, with certain prominent bands signifying complexation (Nakamoto *et al*., 1978). V(M-N) was accountable for the emergence of new bands in the 500–609 cm^{-1}. Consequently, the new bands observed in all the metal complexes suggest that 1,10-phenanthroline coordinated to metal ions via two nitrogen donor atoms of V(C=N) while diphenylmethanonehydrazone was coordinated to metal ions via N, N donor atoms of azomethine V(C=N) and hydrazinic V(N=N) functional groups (Blom *et al*., 1986; Mukai *et al*., 1988).

The assignment of UV-Vis range is given in Table 4, the display of a strong absorbance peak between 200-230 nm in 1,10-phenanthroline diphenylmethanonehydrazone metal complex attributed to the presence of the π→π* electronic transition which is commonly observed in conjugated double bond system or aromatic rings, this band experienced a bathochromic shift in the complexes indication coordination (Gajiwala *et al*., 2025; L Li *et al*., 2025). Results also show broader peak between 250-290 nm in 1, 10-phananthroline diphenylmethanonehydrazone metal complex assigned to n→π* electronic transition, in the complexes, n→π* observed a blue shift (Shi *et al*., 2025). Bands seen between 350 - 380 nm were due to ligand-metal charge transfer (LMCT). The *d-d* transition was recorded in the visible region by concentrating the solution and the band observed at 400 –700 nm, for Fe(II), Ni(II), Mn(II) and Co(II) complexes. These values are in good agreement with the ones reported for distorted octahedral complexes as reported by (Kpomah *et al*., 2018). Zn has filled *d*-subshell, hence do not exhibit *d-d* transitions, bands observed have been interpreted to be charge transfer transition (Toqeer *et al*., 2025).

Table 5 and 6: Antimicrobial activity and Mic data for 1,10-phenanthroline diphenylmethanonehydrazone complexes.

Tables 5 and 6 present the antifungal activity and minimum inhibitory concentration (MIC) values of the synthesized 1,10-phenanthroline diphenylmethanonehydrazone complexes against four pathogenic fungi, allowing a detailed assessment of their inhibitory performance relative to the parent ligand and standard antifungal drugs. The data show clear concentration-dependent inhibition, with higher activity at 200 mg/mL and decreasing inhibition with reduction in concentration.

Table 4: Electronic spectra data (nm) of 1, 10-phenanthroline diphenylmethanonehydrazone complexes

Compound	d^n Configuration	n→π*	π→π*	Charge Transfer	*d-d* Transition
$[Fe(L_1)(L_2)Cl_2]$	d^6	280	200	350	500
$[Zn(L_1)(L_2)Cl_2]$	d^{10}	270	220	350	-
$[Ni(L_1)(L_2)Cl_2]$	d^8	260	220	370	600
$[Mn(L_1)(L_2)Cl_2]$	d^5	250	230	345	400
$[Co(L_1)(L_2)Cl_2]$	d^7	280	250	380	700

Based on microanalytical data and spectral analysis, the structure below has been proposed for the metal complexes **(Fig. 1**)

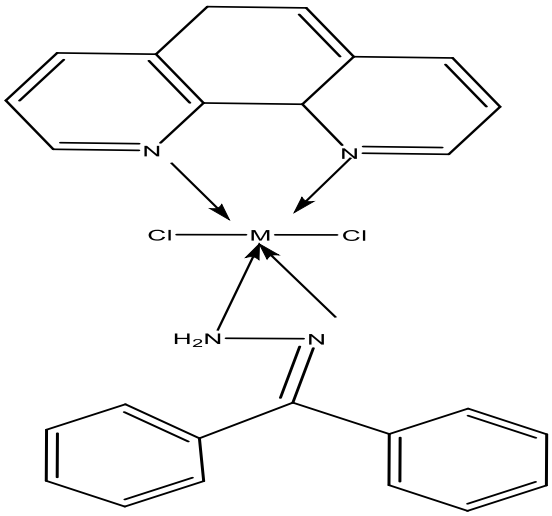

Fig 1. Structure of DPMH metal complexes, where M= Fe (ll), Zn (ll), Ni (ll), Mn (ll), Co (ll).

At 200 mg/mL, all metal complexes exhibited strong susceptibility responses against the four tested fungi, in contrast to the ligand, which showed resistance or intermediate activity. The Fe(II), Zn(II), Ni(II), Mn(II), and Co(II) complexes all produced inhibition zones ranging from 18 to 28 mm, outperforming the standard drugs, particularly against Rhizopus stolonifier, Trichoderma longibbrachiatum, and Candida albicans. Notably, the Ni(II) and Fe(II) complexes recorded the highest inhibition (28 mm), indicating strong fungicidal potential. Compared with the standards, fluconazole and ketoconazole demonstrated moderate to low activity, and intraconazole showed resistance in several cases, further highlighting the superior efficacy of the synthesized complexes.

At 100 mg/mL, the complexes retained appreciable antifungal activity, although inhibition zones decreased slightly. The Ni(II) complex continued to show strong activity with inhibition up to 23 mm, while Fe(II), Zn(II), and Co(II) complexes also maintained susceptibility responses across most fungal strains. The ligand and standard drugs displayed weaker inhibition at this

concentration, reinforcing the enhanced bioactivity conferred by metal coordination.

Table 5: Antifungal Activity (mg/mL) of 1, 10-phenanthroline diphenylmethanone hydrazone complexes

Sample	Concentration	Rhizopus stolonifier	*Trichoderma longibbrachiatum*	*Candidia albican*	*Aspergillus nigri*
DPMH (L1)	200 mg/mL	13 (R)	14 (I)	14 (I)	14 (I)
[Fe(L1)(L2)Cl2]		28 (S)	26 (S)	22 (S)	22 (S)
[Zn(L1)(L2)Cl2]		24 (S)	23 (S)	18 (S)	22 (S)
[Ni(L1)(L2)Cl2]		28 (S)	25 (S)	24 (S)	22 (S)
[Mn(L1)(L2)Cl2]		18 (S)	20 (S)	14 (I)	18 (S)
[Co(L1)(L2)Cl2]		26 (S)	24 (S)	20 (S)	14 (I)
Fluconazole		20 (S)	18 (S)	12 (R)	14 (I)
Intraconazole		18 (S)	16 (S)	14 (I)	12 (R)
Ketoconazole		16 (S)	16 (S)	14 (I)	14 (I)
DPMH (L1)	100 mg/mL	10 (R)	10 (R)	8 (R)	10 (R)
[Fe(L1)(L2)Cl2]		22 (S)	20 (S)	16 (S)	19 (S)
[Zn(L1)(L2)Cl2]		18 (S)	19 (S)	16 (S)	18 (S)
[Ni(L1)(L2)Cl2]		23 (S)	21 (S)	20 (S)	17 (S)
[Mn(L1)(L2)Cl2]		14 (I)	15 (I)	10 (R)	14 (I)
[Co(L1)(L2)Cl2		22 (S)	18 (S)	16 (S)	10 (R)
Fluconazole		15 (I)	14 (I)	6 (R)	10 (R)
Intraconazole		12 (R)	10 (R)	12 (R)	6 (R)
Ketoconazole		12 (R)	10 (R)	10 (R)	12 (R)
DPMH (L1)	50 mg/mL	6 (R)	4 (R)	6 (R)	4 (R)
[Fe(L1)(L2)Cl2]		20 (S)	16 (S)	12 (R)	16 (I)
[Zn(L1)(L2)Cl2]		14 (I)	15 (I)	10 (R)	12 (R)
[Ni(L1)(L2)Cl2]		16 (S)	18 (S)	16 (R)	12 (R)
[Mn(L1)(L2)Cl2]		8 (R)	12 (R)	4 (R)	10 (R)
[Co(L1)(L2)Cl2]		15 (I)	14 (I)	10 (R)	6 (R)

Fluconazole	8 (R)	8 (I)	2 (R)	4 (I)
Intraconazole	4 (S)	4 (R)	4 (R)	2 (R)
Ketoconazole	8 (R)	2 (R)	4 (I)	4 (R)

Table 6: MIC (µg/mL) of Antifungal Activity of 1, 10-phenathroline diphenylmethanone hydrazone complexes

Sample	*Rhizopus stolonifier*	*Trichoderma longibbrachiatum*	*Candidia albican*	*Aspergillus nigri*
DPMH (L1)	35.48	25.11	50	50
[Fe(L1)(L2)Cl2]	15.85	25.11	28.18	25.11
[Zn(L1)(L2)Cl2]	25.11	17.78	25.11	28.18
[Ni(L1)(L2)Cl2]	17.78	31.62	25.11	28.18
[Mn (L1)(L2)Cl2]	35.48	25.11	44.67	28.18
[Co(L1)(L2)Cl2]	25.11	17.78	31.62	35.48
Fluconazole	39.81	35.48	50	44.67
Intraconazole	44.67	39.81	50	50
Ketoconazole	31.62	50	44.67	44.67

At 50 mg/mL, only the Fe(II) and Ni(II) complexes showed susceptibility in most fungi, whereas other complexes exhibited intermediate or resistant responses, indicating reduced potency at lower concentrations. In contrast, the standard drugs showed predominantly resistant behaviour at this concentration, demonstrating that even at reduced doses, some of the synthesized complexes remained more effective than the commercial antifungal agents.

Table 6 complements the inhibition-zone data by presenting MIC values, which provide a direct measure of the minimum concentration required to inhibit fungal growth. The complexes exhibited lower MIC values than the ligand and most standard drugs, confirming their superior antifungal potency. The Fe(II) and Ni(II) complexes displayed the lowest MIC values, with Fe(II) showing 15.85 µg/mL against Rhizopus stolonifier and Ni(II) exhibiting 17.78–31.62 µg/mL across the fungi. These values are significantly lower than those of fluconazole, intraconazole, and ketoconazole, which ranged from 31.62 to 50 µg/mL. Compared with previously reported results, the MIC values observed here are consistent with metal–hydrazone complexes known to enhance ligand bioactivity through improved lipophilicity, chelation-enhanced permeability, and interference with fungal metabolic pathways. For instance, Subhash *et al*. (2024) also reported enhanced antifungal activity for metal–hydrazone complexes, with MIC values comparable to or lower than commercial antifungal agents.

Overall, the results demonstrate that metal coordination significantly improves the antifungal efficiency of diphenylmethanonehydrazone, with Fe(II) and Ni(II) complexes showing the highest potency across all tested strains. The strong activity observed in this study aligns with earlier findings that phenanthroline-based hydrazone complexes exhibit broad-spectrum antifungal activity due to their ability to bind microbial biomolecules, disrupt membrane integrity, and generate reactive species. When compared with existing literature, the synthesized complexes demonstrate similar or greater efficacy,

underscoring their potential as promising antifungal agents with enhanced performance over standard therapeutic drugs.

5.0 Conclusion

This study report successfully synthesized and characterized of Fe(II), Zn(II), Ni(II), Mn(II), and Co(II) mixed-ligand complexes derived from diphenylmethanonehydrazone and 1,10-phenanthroline. The Schiff base ligand was obtained through condensation of hydrazine hydrate and diphenylmethanone in a 1:1 molar ratio, after which the resulting hydrazone coordinated with metal(II) chlorides and 1,10-phenanthroline to form the mixed-ligand complexes in a 1:1:1 stoichiometry. Spectroscopic, elemental, solubility, and melting point analyses confirmed the successful formation of the complexes. The high melting points indicated strong thermal stability, while solubility patterns showed that all compounds were insoluble in water and lower alcohols but soluble in DMSO and DMF. Infrared and UV–visible data further revealed that 1,10-phenanthroline coordinated via its azomethine nitrogen atoms, while diphenylmethanonehydrazone bound through the azomethine (C=N) and hydrazinic (N=N) donor sites. Electronic spectra suggested LMCT bands for the Zn(II) and Mn(II) complexes and d–d transitions in the 500–700 nm region for Fe(II), Ni(II), and Co(II), consistent with octahedral geometry.

The antifungal activity of all synthesized compounds was evaluated against *Aspergillus niger*, *Candida albicans*, *Trichoderma longibbrachiatum*, and *Rhizopus stolonifier*. Most of the mixed-ligand complexes showed higher or comparable activity to the standard antifungal drugs tested. The lowest MIC value (15.85 µg/mL) was recorded for the Fe(II) complex, [Fe(L1)(L2)Cl_2], against *Rhizopus stolonifier*, identifying it as the most potent compound. Generally, the mixed-ligand complexes exhibited superior antifungal.

5.0 References

Ali, I., Khan, S., Toloza, C. A., Shah, Z. A., Iqbal, Z., Ullah, R., & Shah, M. R. (2023). Synthesis, characterizations, and applications of Schiff base functionalized silver nanoparticles. *Journal of Molecular Structure*, 1323, pp. 140587. https://doi.org/10.1016/j.rechem.2023.101160

Ali, M. A., & Livingstone, S. E. (1974). Metal complexes of sulphur–nitrogen chelating agents. *Coordination Chemistry Reviews*, 13, 2–3, pp. 101–132.

Al-Shemary, R. K., Ibrahim, I. H., & Al-Marsomy, N. A. (2016). Synthesis, characterization and biological activity of some mixed ligand complexes of 1,10-phenanthroline and [4-(2-hydroxy-1,2-diphenylethylideneamino)-N-pyrimidin-2-yl benzene sulfonamide] with divalent metal ions. *Al-Mustansiriyah Journal of Science*, 27, 5, pp. 55–63.

Azab, M. E., Rizk, S. A., & Amr, A. E. G. E. (2015). Synthesis of some novel heterocyclic and Schiff base derivatives as antimicrobial agents. *Molecules*, 20, 10, pp. 18201–18218.

Blom, N., Odo, J., Nakamoto, K., & Strommen, D. P. (1986). Resonance Raman studies of metal tetrakis(4-N-methylpyridyl) porphine: Band assignments, structure-sensitive bands, and species equilibria. *The Journal of Physical Chemistry*, 90, 13, pp. 2847–2852.

Borges, A., Saavedra, M. J., & Simões, M. (2015). Insights on antimicrobial resistance, biofilms and the use of phytochemicals as new antimicrobial agents. *Current Medicinal Chemistry*, 22, pp. 2590–2614. https://doi.org/10.2174/0929867322666150530210522

Dadgostar, P. (2019). Antimicrobial resistance: Implications and costs. *Infection and Drug Resistance*, 12, pp. 3903–3910. https://doi.org/10.2147/IDR. S234610

Gajiwala, P. H., Solanki, M. B., & Chhowala, T. N. (2025). Pyrazolone-based metal complex azo dyes: Synthesis, characterization, DFT analysis and in vitro antimicrobial assessment. *Journal of Molecular Structure*, 1352, 144345. https://doi.org/10.1016/j.molstruc.2025.144345

Jain, P., Vishvakarma, V. K., Singh, P., Yadav, S., Kumar, R., Chandra, S., Kumar, D., & Misra, N. (2023). Bioactive thiosemicarbazone coordination metal complexes: Synthesis, characterization, theoretical analysis, biological activity, molecular docking and ADME analysis. *Chemistry & Biodiversity*. https://doi.org/10.1002/cbdv.202300760

Juyal, V. K., Pathak, A., Panwar, M., Thakuri, S. C., Prakash, O., Agarwal, A., & Nand, V. (2023). Schiff base metal complexes as a versatile catalyst: A review. *Journal of Organometallic Chemistry*, 999, pp. 122825. https://doi.org/10.1016/j.jorganchem.2023.122825

Kashar, T. I., & El-Sehli, A. H. (2013). Synthesis, characterization, antimicrobial and anticancer activity of Zn(II), Pd(II) and Ru(III) complexes of dehydroacetic acid hydrazone. *Journal of Chemical and Pharmaceutical Research*, 5, 11, pp. 474–483.

Kpomah, B., Kpomah, E. D., Ugbune, U., Agbaire, P. O., & Apiamu, A. (2024). Reduced toxicity of methylphenyl ketone compounds by combining them with metal ions. *Iranian Journal of Toxicology*, 18, 3, pp. 120–129. http://dx.doi.org/10.32592/ijt.18.3.120

Kpomah, B., Kpomah, E. D., & Ugbune, U. (2018). Transition metal complexes with N,S′ and N,N′ bidentate mixed ligands: Synthesis, characterization and activity. *Applied Science Reports*, 22, 2, pp. 38–44.

Kumar, R., Singh, A. A., Kumar, U., Jain, P., Sharma, A. K., Kant, C., Haque, M. S., & Faizi. (2023). Recent advances in synthesis of heterocyclic Schiff base transition metal complexes and their antimicrobial activities, especially antibacterial and antifungal. *Journal of Molecular Structure*, 1294, pp. 136346. https://doi.org/10.1016/j.molstruc.2023.136346

Lemire, J. A., Harrison, J. J., & Turner, R. J. (2013). Antimicrobial activity of metals: Mechanisms, molecular targets and applications. *Nature Reviews Microbiology*, 11, pp. 371–384.

Lever, A. B. P., & Ozin, G. A. (1977). Electronic spectra of zerovalent hexakis(dinitrogen) and hexacarbonyl derivatives of titanium, vanadium and chromium. *Inorganic Chemistry*, 16, 8, pp. 2012–2016.

Li, G., Du, Z., Wu, C., Liu, Y., Xu, Y., Lavendomme, R., Liang, S., Gao, E., & Zhang, D. (2025). Charge-transfer complexation of coordination cages for enhanced photochromism and photocatalysis. *Nature Communications*, 16, 1, pp. 546. https://doi.org/10.1038/s41467-025-55893-z

Malav, R., & Ray, S. (2025). Recent advances in the synthesis and versatile applications of transition metal complexes featuring Schiff base ligands. *RSC Advances*, 15, 28, pp. 22889–22914. https://doi.org/10.1039/D5RA03626G

Mihsen, H. H., Abass, S. K., Hassan, Z. M., & Abass, A. K. (2020). Synthesis, characterization and antimicrobial activities of mixed ligand complexes of Fe(II), Co(II), Ni(II) and Cu(II) ions derived from imine of benzidine and o-

phenylenediamine. *Iraqi Journal of Science*, pp. 2762–2775.

Muteeb, G., Rehman, M. T., Shahwan, M., & Aatif, M. (2023). Origin of antibiotics and antibiotic resistance, and their impacts on drug development: A narrative review. *Pharmaceuticals*, 16, pp. 1–54. https://doi.org/10.3390/ph16111615

Nakamoto, Y., Asano, Y., Dohi, K., Fujioka, M., Iida, H., Kida, H., & Takeuchi, J. (1978). Primary IgA glomerulonephritis and Schönlein–Henoch purpura nephritis: Clinicopathological and immunohistological characteristics. *QJM: An International Journal of Medicine*, 47, 4, pp. 495–516.

Shi, H., Zhang, H., Li, B., Zhang, Y., & Wei, K. (2025). Structural, spectroscopical, theoretical and antibacterial investigation of anion-regulated dinuclear nickel(II) Salamo-type complexes. *Journal of Molecular Structure*, 1350, pp. 144161. https://doi.org/10.1016/j.molstruc.2025.144161

Subhash, M., Kumar, A., Phor, M., Gupta, A., & Chaudhary. (2024). Design, synthesis, characterization, in vitro cytotoxic, antimicrobial, antioxidant studies, DFT, thermal and molecular docking evaluation of biocompatible Co(II) complexes of N_4O_4 macrocyclic ligands. *Computational Biology and Chemistry*, 110, pp. 108032. https://doi.org/10.1016/j.compbiolchem.2024.108032

Swartz, M. N. (2000). Impact of antimicrobial agents and chemotherapy from 1972 to 1998. *Antimicrobial Agents and Chemotherapy*, 44, pp. 2009–2016.

Tegos, G. P., & Hamblin, M. R. (2013). Disruptive innovations: New anti-infectives in the age of resistance. *Current Opinion in Pharmacology*, 13, pp. 673–677.

Ventola, C. L. (2015). The antibiotic resistance crisis part 1: Causes and threats. *P&T*, 40, 4, pp. 277–283.

Declaration

Funding sources

No funding.

Conflict of Interests

The authors declare that there is no conflict of interest regarding the publication of this paper.

Ethical considerations.

Not applicable

Author's contribution

This work was carried out in collaboration between all authors. Author ELI designed the study, performed all analyses, and wrote the first draft of the manuscript. Authors BK and OA managed the analysis of the study. All authors read and approved the final manuscript.